

**NASA  
Technical  
Paper  
2902**

1989

**Secondary Electron Emission  
Characteristics of Untreated  
and Ion-Textured Titanium**

Arthur N. Curren  
and Kenneth A. Jensen  
*Lewis Research Center*  
*Cleveland, Ohio*

Gary A. Blackford  
*Case Western Reserve University*  
*Cleveland, Ohio*



National Aeronautics and  
Space Administration  
Office of Management  
Scientific and Technical  
Information Division

## Summary

Experimentally determined values of true secondary electron emission and relative values of reflected primary electron yield are presented for untreated (simply machined) and ion-textured, high-purity titanium over ranges of primary electron beam energies and beam impingement angles. The purpose of the investigation was to explore the feasibility of using titanium as electrode material in the multistage depressed collectors (MDC's) used in microwave amplifier traveling wave tubes (TWT's) for space communications and aircraft applications. Because of its relatively low density and thermal expansion characteristics and relatively high strength, thermal emissivity, and melting temperature, titanium presents itself as a possible candidate for the MDC electrode application. A detailed description of the method of ion texturing the titanium is included. Although the ion-treated surface considered in this study is not presented as being optimum from the standpoint of secondary electron emission suppression, it nevertheless serves to demonstrate that the surface can be modified by this procedure to significantly reduce these emission characteristics relative to those of the untreated surface. Further studies can reasonably be expected to produce surfaces with even lower secondary emission characteristics. The titanium surfaces were tested at primary electron beam energies of 200 to 2000 eV and at direct ( $0^\circ$ ) to near-grazing ( $85^\circ$ ) beam impingement angles. True secondary electron emission and relative reflected primary electron yield characteristics of the surfaces were compared with each other and with those of oxygen-free, high-conductivity (OFHC) copper (the material most commonly used for MDC electrodes). The ion-textured titanium surface exhibited secondary electron emission characteristics sharply lower than those exhibited by untreated titanium or copper. Clearly, then, in consideration of the secondary electron emission suppression of ion-textured titanium along with its other favorable physical properties, it must be included as a potential candidate for use as MDC electrode material in some applications.

## Introduction

Because of the limited electrical power available, high overall efficiency is a requirement for microwave amplifier traveling-wave tubes (TWT's) in space communications and

aircraft applications. In addition to advances in cathode and radiofrequency (RF) interaction circuit technology, the development and implementation of the multistage depressed collector (MDC) (ref. 1) has played an important role in the effort to achieve high TWT efficiency. In order to maximize the efficiency of the MDC, in turn, the use of electrode materials having low secondary electron emission characteristics (ref. 2) is necessary. As the spent electron beam enters the MDC from the TWT's RF interaction circuit, the electrons are slowed by a retarding electrical field and are collected selectively by their energies, with relatively small losses. The MDC efficiency is directly influenced by the ability of the electrodes to capture and retain the impinging electrons. Specifically, for the maximum kinetic energy to be recovered from the spent electron beam, the electrode surfaces must have a low secondary electron emission ratio, or ratio of reemitted electrons to impinging electrons, to prevent the electrons from being excessively reflected or reemitted from the electrodes.

The material most commonly used by TWT manufacturers for MDC electrodes is oxygen-free, high-conductivity (OFHC) copper, although that material exhibits relatively high levels of secondary electron emission if its surface is not treated for emission control. Such treatments for OFHC copper include roughening the surface by particle blasting or coating it with materials having lower emission characteristics than those of the base material. It has been shown that ion texturing the OFHC copper surface sharply reduces the emission characteristics (ref. 3) and that the sputter application of highly textured carbon (ref. 4) or the spark-discharge deposition of polycrystalline carbon (ref. 5) on copper reduces the emission characteristics even further.

Another approach to providing MDC electrodes with low secondary electron emission characteristics is to use pyrolytic graphite (ref. 6) or high-purity isotropic graphite (ref. 3), both of which have relatively low emission properties without further treatment. With each of these carbon forms, however, appropriate ion texturing has been shown to reduce the emission characteristics to the lowest levels so far observed. A detailed survey of the use of carbon and carbon-based electrodes for MDC application is presented in reference 7.

Titanium, in part by virtue of its low density and high melting temperature relative to OFHC copper, is of interest as a candidate MDC electrode material. In view of that interest, a sample of machined (but otherwise untreated) high-purity titanium was evaluated for its secondary electron emission

characteristics. Further, a procedure for producing a dense, uniform, highly textured titanium surface by means of ion bombardment was developed, and a sample of that textured material was also evaluated for emission characteristics. Although the ion-textured surface considered in this study is not presented as being optimum from the standpoint of secondary electron emission suppression, it does demonstrate that the titanium surface can be modified by ion texturing to significantly reduce the emission characteristics relative to those of the untreated surface. It is reasonable to assume that further development of the texturing process with this material could lead to surfaces with even lower emission levels.

This report summarizes the experimentally determined secondary electron emission characteristics of untreated (simply machined) and ion-textured titanium over ranges of primary electron beam energies and beam impingement angles representative of the MDC electrode application. Further, limited comparisons of these values with those of OFHC copper are presented so that the reader can comprehensively assess the potential application areas of titanium in this regard.

## Experimental Apparatus, Materials, and Procedures

### Ion Texturing

A schematic of the ion-texturing facility used in this study is shown in figure 1. A detailed description of this apparatus and its operating procedures is presented in reference 6. Briefly, a sample of the material to be treated was positioned in the instrumented receptacle structure shown in the schematic and was subjected to argon ion bombardment in a low-pressure (approx. 2.66 mPa;  $2 \times 10^{-5}$  torr) environment. Operating variables in the procedure were accelerating potential difference between the plasma and the sample, argon flow rate, sample surface current density, and duration of ion bombardment. The titanium sample textured in this study was a disk approximately 2.1 cm (0.828 in.) in diameter by 0.15 cm (0.060 in.) thick. The sample was cleaned immediately before texturing by successively washing it in clean acetone, clean ethyl alcohol, and clean distilled water, followed by air drying.

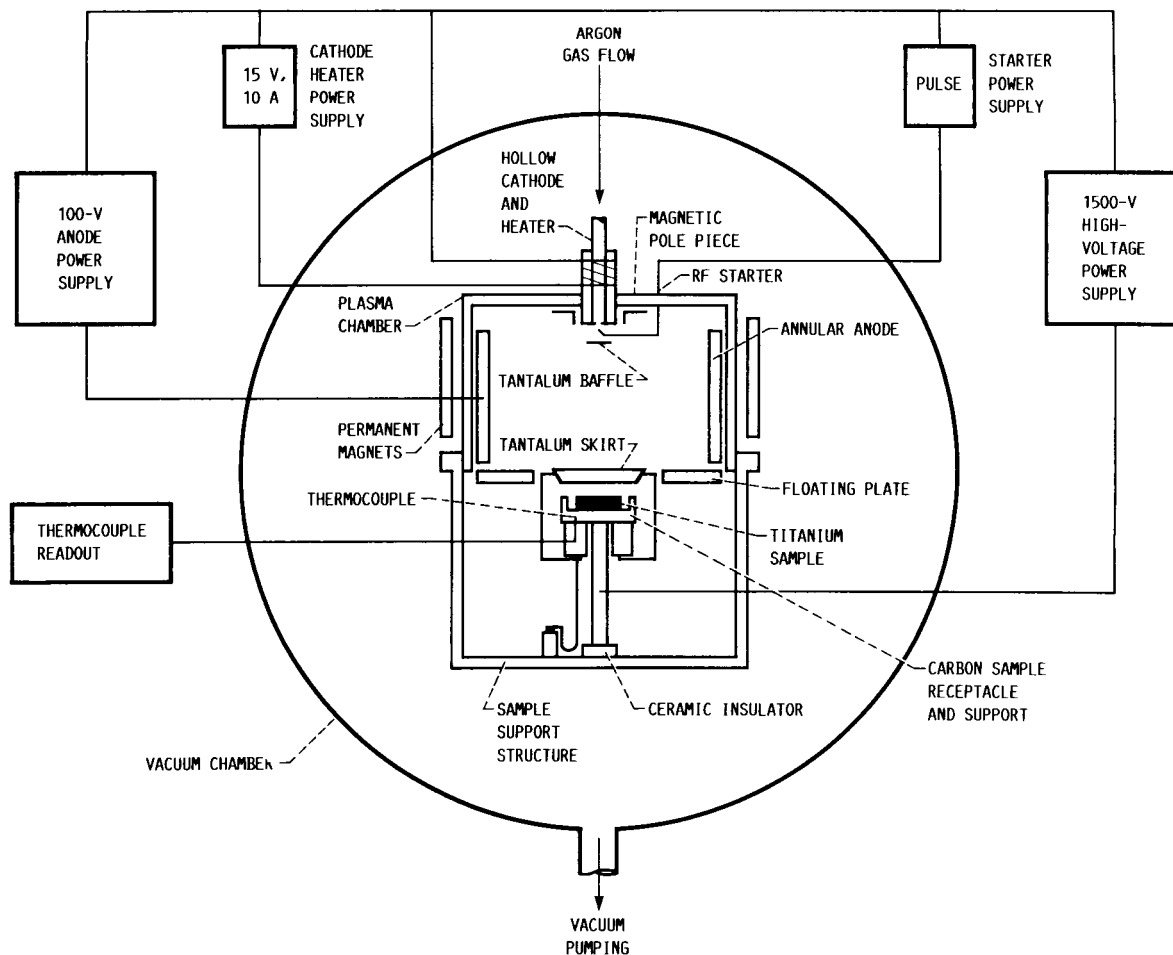


Figure 1.—Schematic of ion-texturing apparatus.

# ORIGINAL PAGE IS OF POOR QUALITY

Figure 2 shows the sample receptacle, which is shown in place schematically in figure 1. Mounted above and surrounding the sample was a narrow pure-tantalum skirt that sloped inward toward the sample at a 45° angle. The inside diameter of the 0.635-cm (0.25-in.) wide skirt was about 4.53 cm (1.785 in.), and the height of the skirt bottom above the level of the sample surface was about 0.795 cm (0.313 in.). The tantalum skirt was necessary to provide a sputtered "seed" or "mask" for the sample surface, since titanium does not spontaneously form

the desired surface structure for secondary electron emission suppression under ion bombardment alone. A material such as tantalum, which has a higher melting temperature than titanium, when arranged and electrically biased properly, "seeds" the titanium surface and causes texturing to occur under ion bombardment. Specifically, for the titanium sample that was ion textured in this study, the accelerating potential difference was 1500 eV, the argon flow rate was 60 std cm<sup>3</sup>/min, the sample surface current density was 5 mA/cm<sup>2</sup>, and the texturing period was 2 hr. During the texturing period a thermocouple located on the sample support structure in contact with the sample indicated that the temperature at that point rapidly rose to and stabilized at 499 °C. The skirt and sample were held at the same potential relative to the plasma during the entire period of ion bombardment. Placement of the seeding material is important for producing uniform and mature ion texturing over the surface configuration to be treated. Depending on the complexity of the surface to be treated, some experimentation with seed material placement and operating procedures may be required to produce uniform and effective texturing over the entire surface.

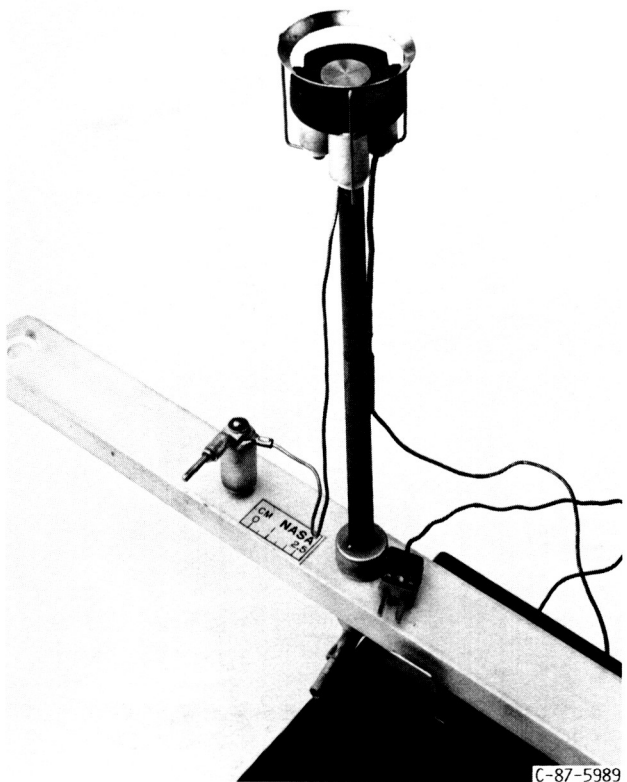


Figure 2.—Sample receptacle and support structure showing titanium sample in position prior to installation in ion-texturing apparatus. (Note tantalum skirt surrounding sample and electrical and thermocouple leads.)

## Titanium

The material investigated in this study, unalloyed titanium, grade 1, ASTM specification B265, has some characteristics that make it an attractive candidate for the MDC electrode application. Table I displays selected properties (taken from refs. 8 and 9) of this high-purity titanium, OFHC copper (the most commonly used material for MDC electrodes), and the high-purity tantalum seeding material. Titanium has a much higher melting temperature and is considerably lighter in weight than OFHC copper, although its thermal conductivity is much lower. Total normal thermal emissivity, an important consideration in MDC thermal control, is much higher for titanium than for OFHC copper. Titanium certainly has adequate physical strength for the MDC electrode application, and its well-known ability to absorb hydrogen, oxygen, and

TABLE I.—SOME SELECTED PROPERTIES OF OFHC COPPER,  
HIGH-PURITY TITANIUM, AND HIGH-PURITY TANTALUM

Property	OFHC copper	High-purity titanium	High-purity tantalum
Density at RT <sup>a</sup> , g/cm <sup>3</sup>	8.94	4.50	16.6
Melting temperature, °C	1083	1675	2996±50
Tensile strength at RT, Pa (psi)	$1.93 \times 10^8$ (28 000)	$2.34 \times 10^8$ (34 000)	-----
Yield strength at RT (for 0.5-percent extension under load), Pa (psi)	$5.45 \times 10^7$ (7900)	$1.72 \times 10^8$ (25 000)	-----
Coefficient of thermal expansion at RT, cm/cm °C	$16.5 \times 10^{-6}$	$8.4 \times 10^{-6}$	$6.5 \times 10^{-6}$
Thermal conductivity at RT, cal/cm <sup>2</sup> cm sec °C	0.934	0.0407	0.13
Specific heat at RT, cal/g °C	0.092	0.125	-----
Total normal thermal emissivity at RT	0.023	0.13	-----
Modulus of elasticity at RT, Pa (psi)	$1.10 \times 10^{11}$ ( $16 \times 10^6$ )	$1.07 \times 10^{11}$ ( $1.55 \times 10^7$ )	-----

<sup>a</sup>RT indicates room temperature.

nitrogen may provide some useful pumping in the vacuum envelope, particularly at elevated temperatures. Importantly, the thermal expansion coefficient is near to those for typical ceramics ( $\text{Al}_2\text{O}_3$ ,  $\text{ZrO}_2$ , and  $\text{BeO}$ ) (ref. 8) to which electrodes are commonly brazed in MDC structures. This characteristic suggests simpler brazing procedures than for situations where greater differences in thermal expansion coefficients occur. For example, brazing OFHC copper electrodes to ceramics requires special measures.

### Tantalum

Some of the properties of tantalum, the "seeding" material used in the titanium ion-texturing process, are also presented in table I. The melting temperature of this metal is well above that of titanium, a requirement for the process, as described in reference 10. Although tantalum is considerably denser than titanium, only insignificant amounts of it are permanently deposited on the titanium during ion texturing (as will be described elsewhere in this study) with no resulting measurable adverse weight effect. Again, because of the very small amount of tantalum remaining on the textured titanium surface, the differences between the thermal expansion coefficients and thermal conductivities of the two metals must reasonably be considered to be unimportant. Although tantalum was the only seeding material included in this study, other metals can probably be used for this purpose.

### Secondary Electron Emission Evaluation

The facilities and procedures used to evaluate the secondary electron emission characteristics of the titanium samples investigated in this study are described in detail in reference 6. Briefly, the samples were attached to a micromanipulator-mounted support fixture and installed in an ultra-high-vacuum vessel equipped with a residual gas analyzer (RGA) and a scanning Auger spectrometer cylindrical mirror analyzer (CMA) that had an integral electron gun. A filament heater-reflector system and a thermocouple were incorporated into the sample-holding fixture for sample degassing and temperature monitoring. The vacuum chamber was evacuated to a pressure of  $13.3 \text{ nPa}$  ( $1 \times 10^{-10} \text{ torr}$ ) or less for testing. During the pumpdown the entire vacuum chamber was heated to about  $250^\circ \text{C}$  for 16 hr to degas the system. After that procedure the samples were heated by filament radiation and electron bombardment to about  $500^\circ \text{C}$  for 3 to 4 hr to further degas the sample and thus simulate the anticipated "bakeout" temperature to which an MDC assembly on a TWT would be subjected. Along with the secondary electron emission measurements, Auger spectroscopic examinations were conducted to determine the chemical compositions of the sample surfaces. These examinations and measurements are discussed in the section "Experimental Results."

The bottom half of each sample disk was coated with soot to provide a control surface. The affected area of the ion-textured sample was smoothed to return the surface as nearly

as possible to the untreated condition before the soot coating was applied. During the evaluation of the sample surfaces for secondary electron emission characteristics, tests were routinely performed at two or more locations on each half of the disk surface. This procedure helped to ensure the validity of the data since the well-known and readily repeatable very low secondary electron emission characteristics of soot provided a "standard" that would immediately reveal errors in procedure or instrument function should they occur.

The surfaces studied in this investigation were evaluated for true secondary electron emission and reflected primary electron yield characteristics at 11 primary electron beam energy levels from 200 to 2000 eV for each of eight beam impingement angles from  $0^\circ$  (directly impinging) to  $85^\circ$  (near grazing). For each angle the electron gun was focused to produce a spot diameter at the sample of about  $10 \mu\text{m}$ . Tests at identical conditions were routinely repeated and yielded repeatable results (within limits of measurement) in every instance. Scanning electron microscope examinations after lengthy periods of testing revealed no observable surface damage from electron beam impingement for any of the surfaces.

**True secondary electron emission.**—In true secondary electron emission, electrons undergo inelastic collisions at or near a solid surface that is undergoing electron bombardment and are emitted from that surface with energies of the order of a few tens of electron volts. A sample-biasing method that is described in detail in reference 6 was employed to determine the true secondary electron emission characteristics of the surface investigated in this study. Briefly, with the electron beam focused on the sample surface at a given beam energy level, the measured sample-to-ground current was taken to be the total beam current minus the secondarily emitted current. When an appropriate positive bias voltage (in this case, 90 V) was then applied to the sample, the true secondary electrons were retained by the sample and the resulting measured sample-to-ground current was taken to be the total beam current. The true secondary electron emission ratio  $\delta$ , or ratio of true secondarily emitted electrons to primary electrons, was calculated by the expression

$$\delta = \frac{I_b - (I_b - I_s)}{I_b}$$

where

$I_b - I_s$  beam current minus secondarily emitted current (0.032 to  $2.6 \mu\text{A}$  in this study)  
 $I_b$  beam current (0.50 to  $4.2 \mu\text{A}$  in this study)

**Reflected primary electron yield.**—Reflected primary electrons are electrons that experience elastic collisions at a solid surface undergoing electron bombardment and are reflected from the surface with energies equal to or very nearly

equal to the primary electron beam energy. The method for evaluating the reflected primary electron yield for the surfaces studied in this investigation was adapted from that used in reference 11. The Auger CMA was used to characterize the reflected primary yield at each primary electron beam energy level investigated. The quantity used as a measure of the relative values of reflected primary yields from different surfaces at a given primary electron beam energy and impingement angle was the "reflected primary electron yield index." This is the ratio of the amplitude of the elastic energy peak for a given surface and a given primary electron energy to the amplitude of the elastic energy peak for the control soot surface at the same beam impingement angle and a primary electron beam energy of 1000 eV. The reflected primary electron yield index  $\pi$  is given by

$$\pi = \frac{D_{\text{sample}}}{D_{\text{control}}}$$

where

$D_{\text{sample}}$  elastic curve amplitude for sample surface at a given primary electron beam energy

$D_{\text{control}}$  elastic curve amplitude for soot control surface at 1000-eV primary electron beam energy

As has been stated, soot was selected for the control surface, as it was in reference 11, because of its known extremely low secondary electron emission characteristics and its ability to be readily reproduced. Although this method does not determine the absolute value of the reflected primary electron yield, it serves the important purpose of permitting comparison of this property for different surfaces.

Note that the primary electron yield measured and reported in this study was based only on those electrons that were reflected directly at or very nearly directly at the Auger CMA, which contained the primary electron source. This is also the most important direction of emission from the standpoint of MDC efficiency.

## Experimental Results

### Surfaces Investigated

Scanning electron microscope photomicrographs of the surfaces studied in this investigation are shown in figures 3 and 4. The untreated, or simply machined, titanium surface is shown in figure 3. This surface had no major projections, but the machining process caused some gouging and tearing of the metal. Some small radial scratch-like indentations also appear on the surface and are likely the results of postmachining handling. This surface can reasonably be considered as typical for untreated metals used as electrodes in practical MDC electrode applications. The ion-textured

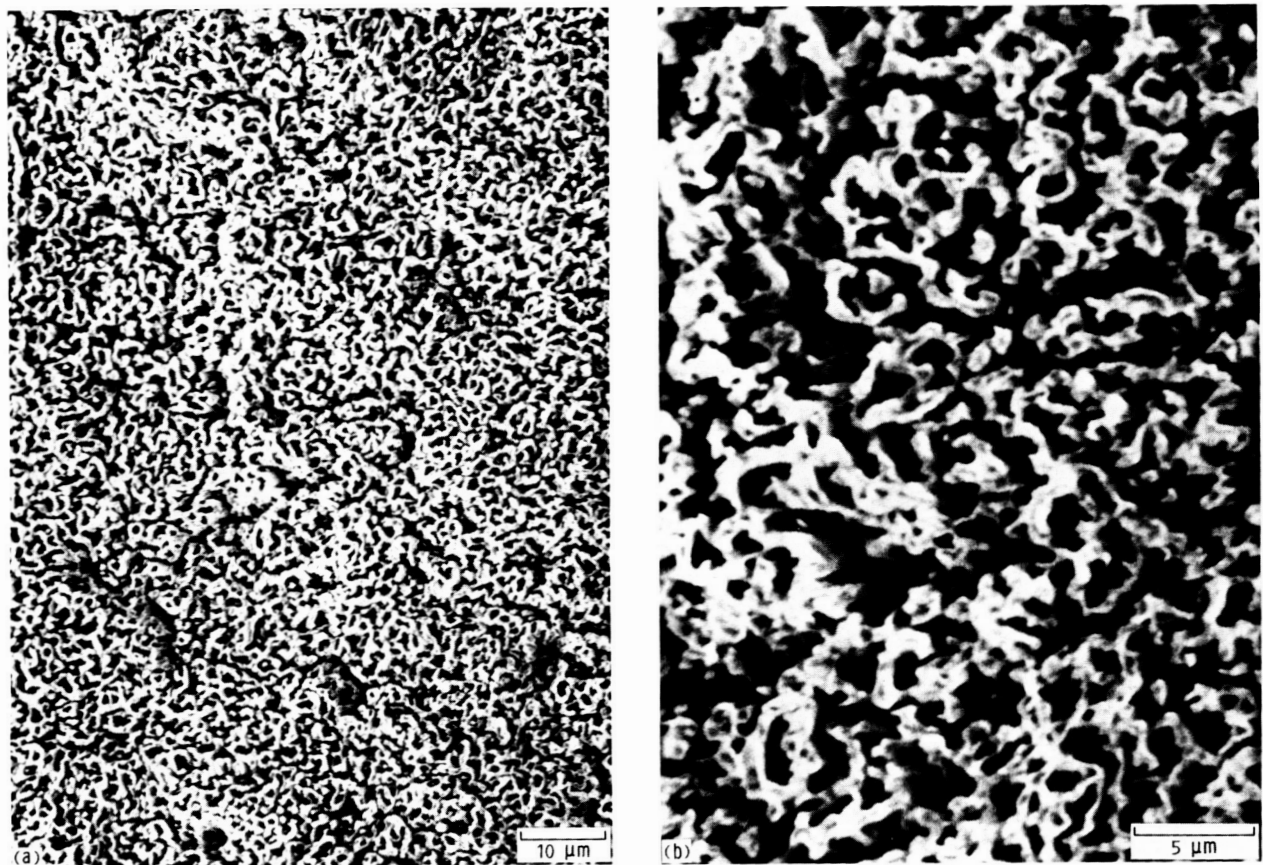


Figure 3.—Untreated (simply machined) titanium surface. (Original photomicrograph taken at magnification of 1000 at 30° angle with surface.)

titanium surface is shown in figure 4(a) at the same magnification as the untreated titanium surface. The texture appears to be dense and uniform over the entire surface, with some slight depressions that are probably due to corresponding depressions in the substrate. Figure 4(b), a photomicrograph of the same surface at a much higher magnification, offers a more detailed view, revealing the coral-like texture more clearly. The walls of the raised texture are essentially vertical, and the average height and spacing between ridges appear to be about 10 and 5  $\mu\text{m}$ , respectively.

Ion texturing the surface of titanium in the manner described in this study markedly changes its general physical appearance as well as its microscopic appearance. Figure 5 displays untreated and ion-textured samples adjacent to each other for comparison. The textured surface appears much darker because of the light-absorbing effect of the projected ridges and the depressions between them.

The ion-textured titanium surface may be damaged or destroyed by vigorous mechanical abrasion but is quite resistant to damage when handled with the care normally afforded materials and components used in TWT fabrication.



(a) Original magnification, 1000.  
(b) Original magnification, 3130.

Figure 4.—Ion-textured titanium surface. (Original photomicrographs taken at 30° angle with surface.)

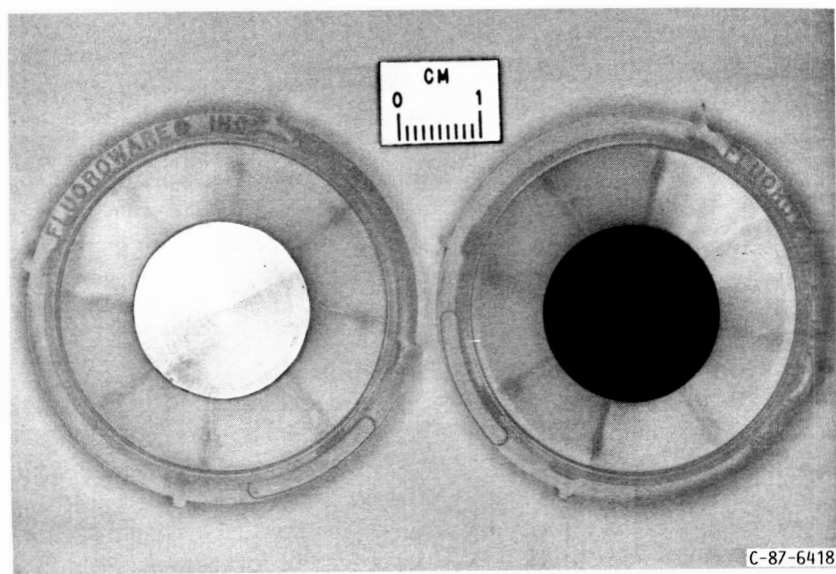


Figure 5.—Contrast in appearance of untreated titanium (left) and ion-textured titanium surfaces. (Samples are shown in storage containers.)

## Sample Surface Auger Examinations

Auger spectrographic examinations were performed for each sample surface studied both before and after the samples were baked out for degassing at 500 °C for several hours. The resulting Auger spectra for the untreated and ion-textured titanium surfaces are presented in figure 6. The instrument sensitivity settings were identical for each examination. Many similarities exist among the spectra, but some important differences are evident, particularly between the pre- and postbakeout plots for each sample.

The major elements present in each prebakeout Auger plot are titanium, carbon, and oxygen. In the postbakeout plots significantly reduced amounts of carbon and oxygen (probably carbon monoxide) are indicated along with higher peak amplitudes for titanium. The highly reactive characteristics of titanium cause it to absorb gases from its environment, principally hydrogen, oxygen, and nitrogen. Heating titanium in vacuum may drive off hydrogen, but oxygen and nitrogen cannot be removed by this method once they have been absorbed (ref. 8). Consequently, we assumed that the reduced amounts of carbon and oxygen in the postbakeout Auger spectra for both the untreated and ion-textured titanium samples must have come about from the partial removal of the carbon oxides layer from the surface during the bakeout procedure. This explanation would also account for the

increased indication of titanium and the appearance of sulfur in the postbakeout plots, since they previously were masked by the now-diminished carbon oxides layer. (The sulfur is attributed to the inadvertent use of a sulfur-bearing cutting oil during the sample fabrication process.) Apparently much of the sulfur on the machined titanium surface was sputtered away during the texturing process, since it is much less evident on the Auger plot for the ion-textured sample than on that for the untreated one. Perhaps a longer or higher-temperature bakeout would further desorb the adsorbed gases, although the bakeout procedure used here is typical for an MDC processed with a TWT.

Note that the presence of tantalum, the texture-inducing seeding material, is not readily apparent on the prebakeout Auger plot for the ion-textured titanium sample and appears only as a very minor indication on the postbakeout surface. We assumed that the tantalum was also masked in the prebakeout examination by the surface layer of carbon oxides but was revealed when the layer was partially removed during bakeout. This observation reinforces the assumption indicated elsewhere in this study that the amount of tantalum permanently deposited on the titanium during ion texturing is insignificantly small.

Although the postbakeout Auger examination for the ion-textured titanium sample displayed significant decreases in carbon and oxygen relative to the prebakeout study, the

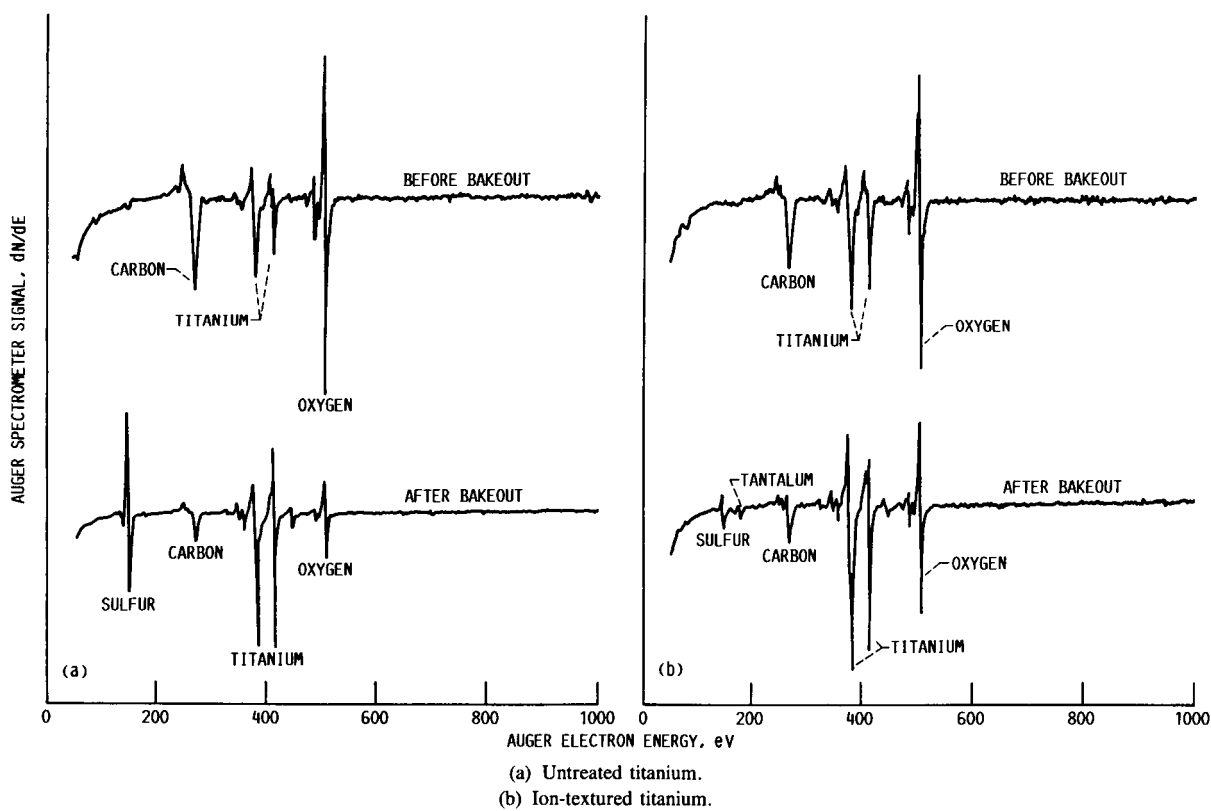


Figure 6.—Pre- and postbakeout Auger spectra for untreated and ion-textured titanium.

decreases are not as prominent as those for the same elements in a similar comparison for the untreated sample. The marked increase in surface area and general configuration complexity of the textured surface apparently resulted in a slower outgassing process than for the relatively simple untreated surface in the same processing environment.

### Secondary Electron Emission Measurements

The experimental results presented in this study are not average or mean values for several "identical" test conditions but are specific values for one test series performed on each surface examined and are considered to be typical for that surface. A relatively large number of similar test series have been performed with titanium and other materials to form the basis for that judgment. Scanning electron microscope examinations were conducted for each sample prior to testing to ensure uniform surface conditions and to reduce the possibility of inadvertently selecting an unusual or atypical location for testing. Neither the ion-texturing procedure described nor the test results achieved in this study are presented as being optimum from the standpoint of secondary electron emission suppression. Rather, the objective of this study is to demonstrate that titanium can be ion textured to effectively reduce its surface secondary electron emission characteristics relative to those of untreated titanium. Further development can reasonably be expected to result in even greater reductions in these emission characteristics for ion-textured titanium.

### True Secondary Electron Emission Ratio

For both the titanium surfaces studied in this investigation, as well as the untreated OFHC copper surface included for comparison, the true secondary electron emission ratio  $\delta$  generally increased with increasing electron beam impingement angle, from direct ( $0^\circ$ ) to near grazing ( $85^\circ$ ), at all points over the primary electron energy range examined. This is illustrated in figures 7(a), 8(a), and 9(a), where the true secondary electron emission ratio for the individual surfaces is plotted as a function of primary electron energy for each of the electron beam impingement angles examined. For the untreated OFHC copper surface (fig. 7(a)), the secondary electron emission characteristics of which were reported in reference 3, the tendency for the true secondary electron emission ratio to increase is attributed to the impinging primary electrons penetrating to decreasing distances below the material surface as the beam impingement angle is increased. The electrons undergoing inelastic collisions then have shorter distances to travel to escape the surface and therefore do so in increasing numbers as the beam angle is increased. The same explanation is taken here to be valid for the characteristics of the untreated titanium surface.

The increase in true secondary electron emission ratio with electron beam impingement angle for the ion-textured titanium surface studied (fig. 9(a)) is in agreement with the reported characteristics of ion-textured, high-purity isotropic graphite,

OFHC copper, and pyrolytic graphite (refs. 3 and 6) as well as textured carbon on OFHC copper (ref. 4). The referenced surfaces are all characterized by dense arrays of randomly positioned individual spires or blunt peaks. As noted elsewhere in this study, the microscopic structure on the surface of the ion-textured titanium (fig. 4) has a ridged, coral-like appearance. The ion-textured titanium can be considered to be similar to the referenced surfaces, except that in this case many closely grouped multiple blunt peaks coalesce with other nearby peaks to form continuous strands of varying width and random lengths. For the ion-textured titanium as well as the other referenced ion-textured surfaces, with a direct ( $0^\circ$ ) electron beam impingement angle, many of the electrons strike the peak walls or base locations. Many of the true secondary electrons generated in those locations then are repeatedly intercepted by the nearby peak walls, reducing the net emission from the projected surface area. As the electron beam impingement angle is increased, beam penetration into the complex surface structure is reduced. The resulting reduced secondary electron trapping effect permits the net true secondary electron emission to increase.

The true secondary electron emission ratio for untreated titanium (fig. 8(a)) exhibited moderately lower levels than that for untreated OFHC copper (fig. 7(a)) over the range of parameters studied. The emission ratio for ion-textured titanium (fig. 9(a)), however, clearly exhibited the lowest ratio of the three surfaces compared at all beam impingement angles and primary electron energies investigated. Compared with the emission ratio characteristics for untreated titanium, the ion-textured titanium displayed essentially a 50 percent reduction in ratio over almost the entire ranges of beam impingement angle and electron energy studied in this investigation.

### Reflected Primary Electron Yield

Curves presenting the reflected primary electron yield index  $\pi$  as a function of primary electron beam energy and beam impingement angle for untreated OFHC copper and untreated titanium are shown in figures 7(b) and 8(b), respectively. As noted elsewhere in this study, the untreated sample surfaces were not lapped or polished but were simply machined to best simulate electrode surfaces commonly used in MDC assemblies. With increasing primary electron beam impingement angle, the electrons that experience elastic collisions with these relatively smooth surfaces reflect increasingly in directions away from the Auger CMA. This then results in progressively smaller measurements of reflected primary electron yield, the general trend of which is shown in figures 7(b) and 8(b). These figures display some departures from the general trend that are here attributed to tiny scratches in the machined surfaces (see fig. 3 as typical). The impinging electron beam apparently interprets these scratches as minute deviations from the average sample surface interaction angle.

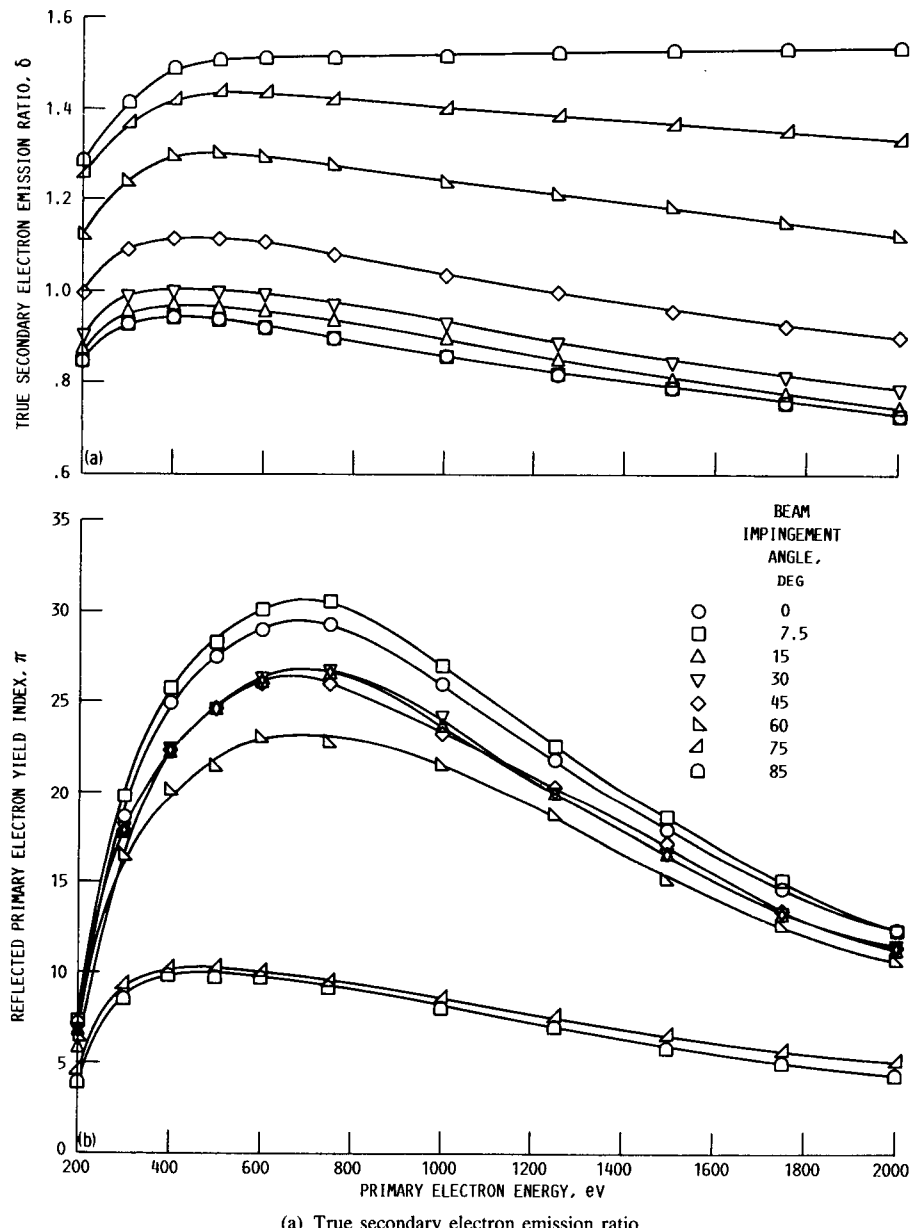


Figure 7.—Characteristics of untreated copper surface as function of primary electron energy.

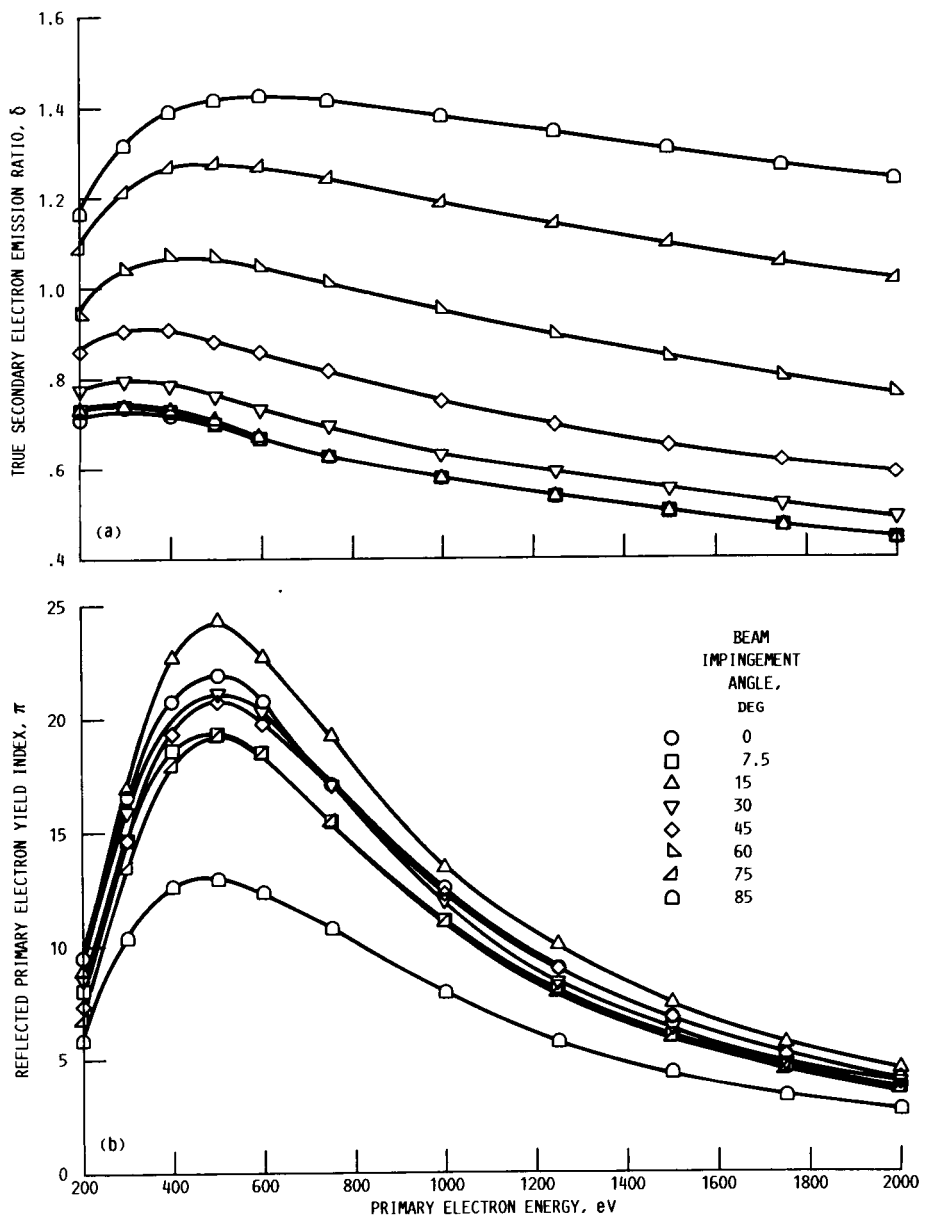


Figure 8.—Characteristics of untreated titanium surface as a function of primary electron energy.

The reflected primary electron yield index for ion-textured titanium, plotted as a function of electron beam energy and beam impingement angle, is shown in figure 9(b). The yield index for this surface is principally a function of beam energy and displays only a very limited variation with beam impingement angle over the range of parameters studied. This lack of sensitivity to beam impingement angle is in contrast to the results of similar studies of ion-textured graphite, ion-textured OFHC copper, and textured carbon on OFHC copper (refs. 3, 4, and 6). In those investigations, in addition to the influence of beam energy, the reflected primary electron yield index was found to be a relatively strong and well-defined function of electron beam impingement angle. This strong impingement angle influence in the referenced studies was attributed to the progressively increasing spire or peak wall surface area presented normal to the Auger CMA as the impingement angle for those surfaces was increased. For the ion-textured titanium surface considered here (fig. 4), the texture configuration apparently was such that the normal projected surface area

presented to the Auger CMA was reasonably constant as the beam impingement angle was increased from direct ( $0^\circ$ ) to near grazing ( $85^\circ$ ), resulting in the yield index results shown in figure 9(b). Again note that modifications in the ion-texturing procedures for titanium employed in this study may cause significant changes in the texture features as well as the true secondary electron emission ratio and reflected primary electron yield characteristics shown in figure 9.

In parallel with the comparisons of the true secondary electron emission ratios for the surfaces studied, the reflected primary electron yield index for the untreated titanium (fig. 8(b)) displayed moderately lower levels than those for untreated OFHC copper (fig. 7(b)) over the range of electron beam energies and beam impingement angles investigated. The reflected primary electron yield index for ion-textured titanium (fig. 9(b)), however, was sharply lower than that of the untreated titanium over essentially the entire range of electron beam energies and beam impingement angles included in this study. This difference was greatest at the lower primary

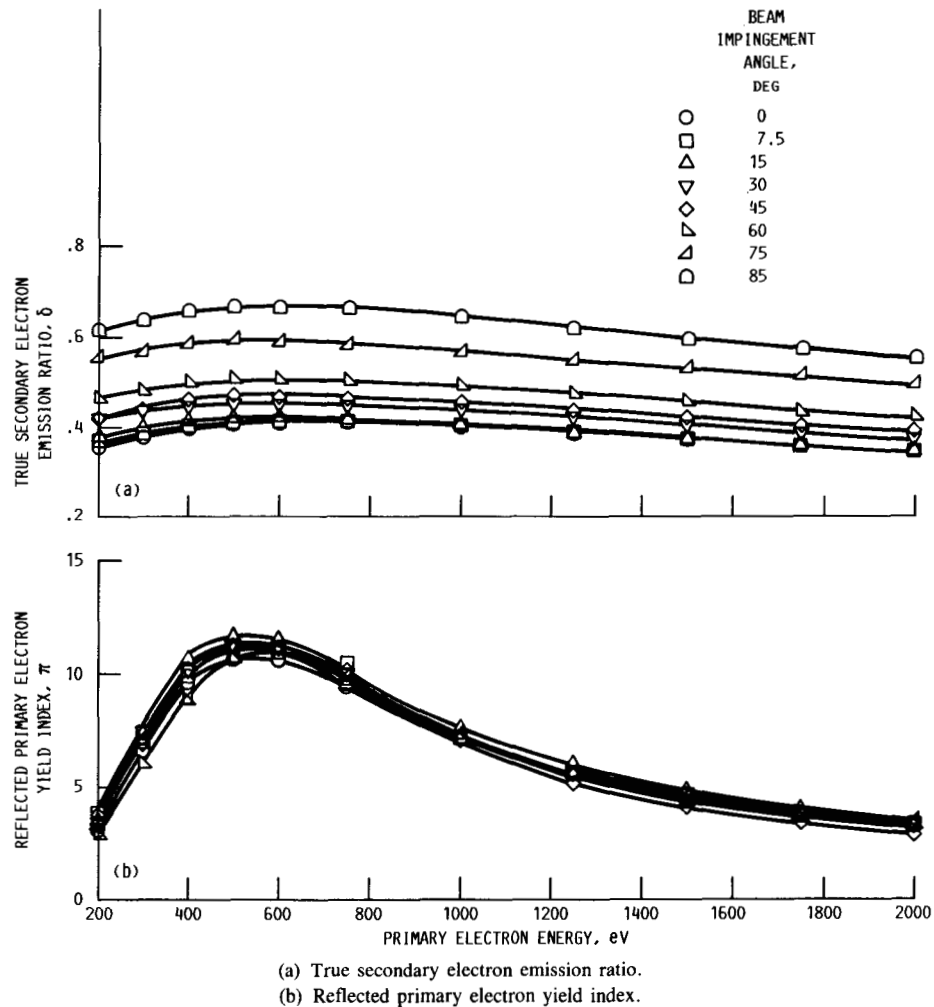


Figure 9.—Characteristics of ion-textured titanium surface as a function of primary electron energy.

electron beam energy levels investigated. Compared with the reflected primary electron yield index of untreated titanium, the yield index of ion-textured titanium displayed a reduction of as much as 50 percent up to about 1000-eV primary beam energy.

### Sample Bakeout Effects on Secondary Electron Emission

Both the untreated and ion-textured titanium surfaces studied in this investigation displayed significant differences between secondary electron emission characteristics measured before and after the sample bakeout or degassing procedure described elsewhere in this study. The prebakeout secondary emission measurements were made at the same time as the prebakeout Auger spectra shown in figure 6 were taken. Although the prebakeout information is not directly useful from the standpoint of actual TWT or MDC operation, it nevertheless

demonstrates the effects of the bakeout process on secondary electron emission properties and is therefore included here. The characteristic changes are presented graphically in figure 10, where the true secondary electron emission ratio and the reflected primary electron yield index are plotted for direct ( $0^\circ$ ) electron beam impingement against primary electron energy over the range 200 to 2000 eV for both pre- and postbakeout sample conditions. The figure clearly shows relatively uniform decreases in true secondary electron emission for each surface as a result of the bakeout process (fig. 10(a)) but equally uniform increases in reflected primary electron yield index from the degassing (fig. 10(b)). The presence of significant amounts of carbon and oxygen on the sample surfaces before degassing is shown in the Auger spectra presented in figure 6. According to the speculation in reference 11, these light atomic weight elements display very low

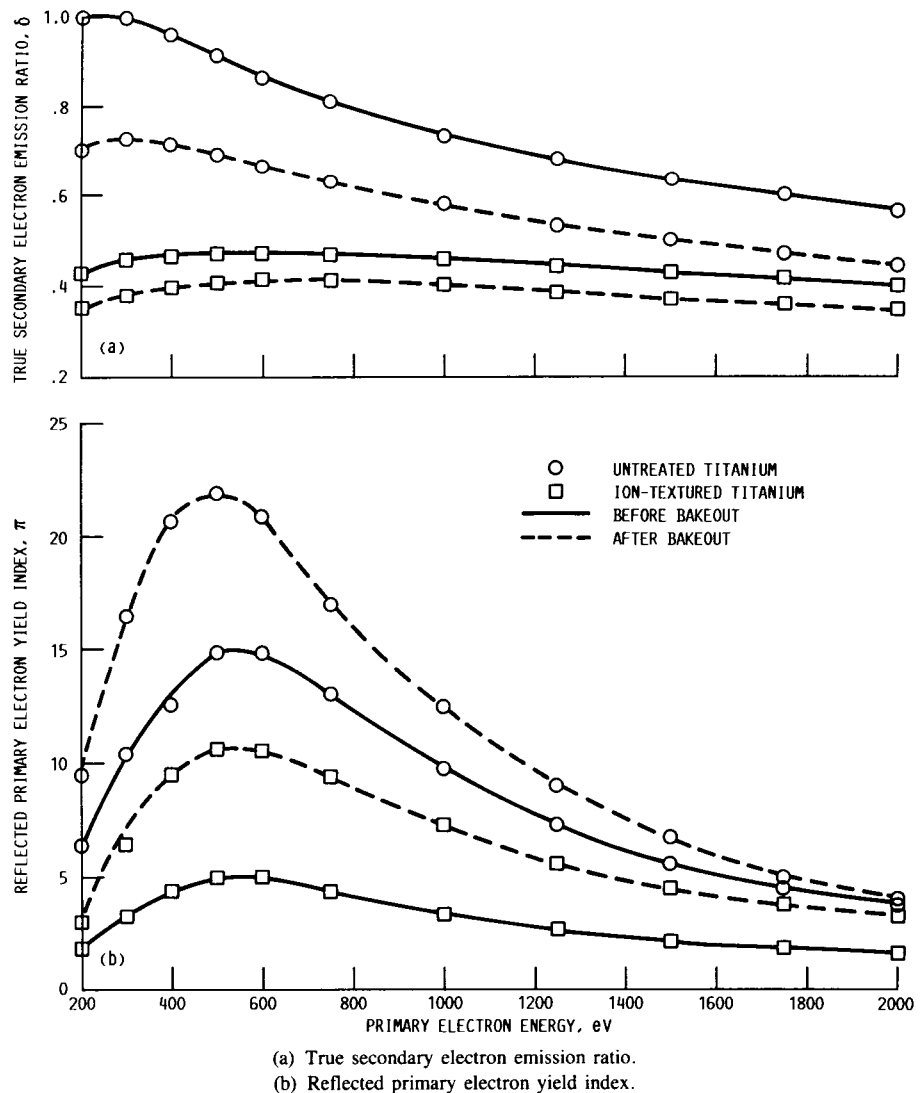


Figure 10.—Characteristics of untreated and ion-textured titanium surfaces before and after 500 °C bakeout. Electron beam impingement angle,  $0^\circ$ .

reflected primary yield and dominate the primary yield effect because the high-energy secondary electrons are probably generated in a surface layer about as thick as the contaminant gas surface layer. When the oxygen and carbon were partially removed by degassing (fig. 6), the reflected primary electrons proportionally increased in number (fig. 10(b)) as the characteristics of the titanium become more dominant. Extending the speculation, it may be reasonable to assume that the prebakeout contaminant layer attenuated some of the high-energy electrons impinging the titanium surface, which were then emitted as lower-energy true secondary electrons. Then, after the layer of contaminants was partially removed by degassing (fig. 6), the true secondary electron emission decreased (fig. 10(a)) as the reflected primary electron yield index increased (fig. 10(b)).

## Conclusions

True secondary electron emission and relative reflected primary electron yield characteristics of untreated and ion-textured titanium were experimentally determined and compared with those of an oxygen-free, high-conductivity (OFHC) copper surface. The ion-textured surface was prepared and the evaluations were done in-house at the NASA Lewis Research Center. The surfaces were tested over a range of primary beam energies from 200 to 2000 eV and at electron beam impingement angles from direct ( $0^\circ$ ) to near grazing ( $85^\circ$ ). The purpose of the investigation was to explore the feasibility of using titanium for electrodes in multistage depressed collectors (MDC's) for high-efficiency microwave amplifier traveling-wave tubes (TWT's) in space communications and aircraft applications. For high efficiency to be attained in MDC's the electrode surfaces must have low secondary electron emission characteristics. The untreated OFHC copper surface was used as a basis for comparison for the titanium surfaces examined because that copper material is commonly used as MDC electrode material.

The secondary electron emission characteristics of the untreated titanium displayed only small differences from those of untreated OFHC copper over the ranges of primary electron beam energy and beam impingement angles tested. The emission characteristics of the ion-textured titanium sample tested, however, were sharply lower (by as much as 50 percent) than those of either of the untreated sample surfaces.

Because of the low emission characteristics, coupled with its relatively high melting temperature, high strength, and total normal thermal emissivity as well as its good gas absorption capability, ion-textured titanium may well be considered as a candidate for high-efficiency MDC electrode applications. Further, it is reasonable to assume that continued development of the ion-texturing procedure employed in this study can result in treated titanium surfaces with even lower secondary electron emission characteristics.

Lewis Research Center  
National Aeronautics and Space Administration  
Cleveland, Ohio, November 29, 1988

## References

1. Kosmahl, H.G.: A Novel, Axisymmetric, Electrostatic Collector for Linear Beam Microwave Tubes. NASA TN D-6093, 1971.
2. Kosmahl, H.G.; and Ramins, P.: Small-Size 81- to 83.5-Percent Efficient 2- and 4-Stage Depressed Collectors for Octave-Bandwidth High-Performance TWT's. IEEE Trans. Electron Devices, vol. ED-24, no. 1, Jan. 1977, pp. 36-44.
3. Curren, A.N.; and Jensen, K.A.: Secondary Electron Emission Characteristics of Ion-Textured Copper and High-Purity Isotropic Graphite Surfaces. NASA TP-2342, 1984.
4. Curren, A.N.; and Jensen, K.A.: Textured Carbon on Copper: A Novel Surface With Extremely Low Secondary Electron Emission Characteristics. NASA TP-2543, 1985.
5. Ebihara, B.T.; Ramins, P.; and Peet, S.: Traveling-Wave-Tube Efficiency Improvement by a Low-Cost Technique for Deposition of Carbon on Multistage Depressed Collector. NASA TP-2719, 1987.
6. Curren, A.N.; and Jensen, K.A.: Beam Impingement Angle Effects on Secondary Electron Emission Characteristics of Textured Pyrolytic Graphite. NASA TP-2285, 1984.
7. Curren, A.N.: Carbon and Carbon-Coated Electrodes for Multistage Depressed Collectors for Electron Beam Devices—A Technology Review. IEEE Trans. Electron Devices, vol. ED-33, no. 11, Nov. 1986, pp. 1902-1914.
8. Kohl, W.H.: Handbook of Materials and Techniques for Vacuum Devices. Reinhold Publishing Corp., 1967.
9. Metals Handbook. Ninth Edition, Vol. 3, American Society of Metals, Metals Park, OH, 1980.
10. Wehner, G.K.; and Hajicek, D.J.: Cone Formation on Metal Targets During Sputtering. J. Appl. Phys., vol. 42, no. 3. Mar. 1, 1971, pp. 1145-1149.
11. Forman, R.: Secondary-Electron-Emission Properties of Conducting Surfaces With Application to Multistage Depressed Collectors for Microwave Amplifiers. NASA TP-1097, 1977.



## Report Documentation Page

1. Report No. NASA TP-2902	2. Government Accession No.	3. Recipient's Catalog No.	
4. Title and Subtitle  Secondary Electron Emission Characteristics of Untreated and Ion-Textured Titanium		5. Report Date  March 1989	
7. Author(s)  Arthur N. Curren, Kenneth A. Jensen, and Gary A. Blackford		6. Performing Organization Code	
9. Performing Organization Name and Address  National Aeronautics and Space Administration Lewis Research Center Cleveland, Ohio 44135-3191		8. Performing Organization Report No.  E-4495	
12. Sponsoring Agency Name and Address  National Aeronautics and Space Administration Washington, D.C. 20546-0001		10. Work Unit No.  506-44-21	
15. Supplementary Notes  Arthur N. Curren and Kenneth A. Jensen, Lewis Research Center; Gary A. Blackford, Case Western Reserve University, Cleveland, Ohio 44106.		11. Contract or Grant No.	
16. Abstract  Experimentally determined values of true secondary electron emission and relative values of reflected primary electron yield are presented for untreated (simply machined) and ion-textured, high-purity titanium over ranges of primary electron beam energies and beam impingement angles. The purpose of the investigation was to explore the feasibility of using titanium as electrode material in the multistage depressed collectors (MDC's) used in microwave amplifier traveling wave tubes (TWT's) for space communications and aircraft applications. Because of its relatively low density and thermal expansion characteristics and relatively high strength, thermal emissivity, and melting temperature, titanium presents itself as a possible candidate for the MDC electrode application. A detailed description of the method of ion texturing the titanium is included. Although the ion-treated surface considered in this study is not presented as being optimum from the standpoint of secondary electron emission suppression, it nevertheless serves to demonstrate that the surface can be modified by this procedure to significantly reduce these emission characteristics relative to those of the untreated surface. Further studies can reasonably be expected to produce surfaces with even lower secondary emission characteristics. The titanium surfaces were tested at primary electron beam energies of 200 to 2000 eV and at direct (0°) to near-grazing (85°) beam impingement angles. True secondary electron emission and relative reflected primary electron yield characteristics of the surfaces were compared with each other and with those of oxygen-free, high-conductivity (OFHC) copper (the material most commonly used for MDC electrodes). The ion-textured titanium surface exhibited secondary electron emission characteristics sharply lower than those exhibited by untreated titanium or copper. Clearly, then, in consideration of the secondary electron emission suppression of ion-textured titanium along with its other favorable physical properties, it must be included as a potential candidate for use as MDC electrode material in some applications.			
17. Key Words (Suggested by Author(s))  Secondary electron emission Titanium Tantalum Traveling-wave tubes	18. Distribution Statement  Unclassified—Unlimited Subject Category 26		
19. Security Classif. (of this report) Unclassified	20. Security Classif. (of this page) Unclassified	21. No of pages 17	22. Price* A03